

Magnetic Capacitance in Variable-Valence Manganese Sulfides

Sergey S. Aplesnin, Anton M. Kharkov,* and Gleb Yu Filipson

The permittivity of $Tm_xMn_{1-x}S$ ($0 < x < 0.15$) solid solutions is measured in the frequency range of 10^2 – 10^6 Hz at temperatures of 300–500 K in magnetic fields of up to 12 kOe. The migration and relaxation conductivity contributions to the electric polarization are established. The relaxation time and activation energy are calculated using the Debye model. A decrease in the capacitance and relaxation time in a magnetic field is observed. The electron polarization relaxation channel provided by recombination of the electron–hole pairs is found using the infrared spectroscopy investigations.


1. Introduction

The magnetoelectric^[1,2] and multiferroic^[3,4] materials with the interplay of the magnetic and electrical properties are interesting for both fundamental research and application. Particular attention is focused on the materials that exhibit the magnetoelectric properties at room and higher temperatures because they can be used in microelectronic data storage systems. Among these materials is the well-studied bismuth ferrite $BiFeO_3$.^[5,6] The giant magnetic capacitance effect observed in $LuFe_2O_4$ ^[7] at room temperature was attributed to the charge fluctuation at different spin values in Fe^{2+} and Fe^{3+} ions due to the elimination of degeneracy between two types of the charge order by an external magnetic field.

The magnetic capacitance in an electrically inhomogeneous medium can be induced by the Maxwell–Wagner effect^[8] due to the tensor nature of the interaction of carriers with magnetic and electric fields and mixing of the longitudinal and transverse conductivity components. In the proposed model, the magnetic capacitance is positive if the size of an electric inhomogeneity is greater than the mean electron free path by an order of magnitude, the measurement time $1/\omega$ is longer than the scattering time, and the matrix is dielectric.^[9]

Prof. S. S. Aplesnin
Kirensky Institute of Physics
Federal Research Center KSC SB RAS
Akademgorodok 50 bld. 38, Krasnoyarsk 660036, Russia

Dr. A. M. Kharkov, G. Yu. Filipson
Institute of Space Technology
Reshetnev Siberian State University of Science and Technology
Krasnoyarskiy rabochiy Ave., 31, Krasnoyarsk 660037, Russia
E-mail: khark.anton@mail.ru

 The ORCID identification number(s) for the author(s) of this article can be found under <https://doi.org/10.1002/pssb.201900637>.

DOI: 10.1002/pssb.201900637

It is still unclear how the magnetic capacitance changes in electrically inhomogeneous semiconductors with the compensation of the charge in the regions with the chemical phase separation. In this case, it is necessary to consider the mobility of electrons and holes, the Coulomb interaction, and the recombination of charges. In the $Tm_xMn_{1-x}S$ solid solutions, the magnetoimpedance was detected above room temperature; in particular, an increase in the reactive part of impedance in a magnetic field was observed.^[10] This effect can be

related to a change in the capacitance and inductance of a sample under the action of a magnetic field.

The aim of the study is to establish the electric polarization type, relaxation mechanism, effect of a magnetic field on the dielectric characteristics, and dielectric loss upon electron doping of semiconductors, depending on the size of an electric inhomogeneity, which is determined by the concentration of ions of different valence.

2. Results and Discussion

The permittivity and dielectric loss were determined by measuring the capacitance and dissipation factor with an AM-3028 component analyzer in the frequency range of 10^2 – 10^6 Hz at temperatures of 300–500 K. The magnetic capacitance $\delta Re(\epsilon)$ and dielectric loss in magnetic field of a sample were determined as

$$\begin{aligned}\delta Re(\epsilon) &= \frac{Re\epsilon(H) - Re\epsilon(0)}{Re\epsilon(0)}; \\ \delta Im(\epsilon) &= \frac{Im\epsilon(H) - Im\epsilon(0)}{Im\epsilon(H)}\end{aligned}\quad (1)$$

where $Re\epsilon(H)$ and $Im\epsilon(H)$ are real and imaginary parts of the permittivity of the sample in a magnetic field of $H = 12$ kOe applied parallel to the capacitor plates and $Re\epsilon(0)$ is in zero magnetic field. To prevent leakage currents, a mica layer with a thickness of several micrometers was placed between the sample and capacitor plates.

Using the frequency dependence of the permittivity, we can determine the time and mechanism of the relaxation of dipole moments. Preventing the leakage current makes it possible to estimate the contribution of the migration polarization caused by charges in the region with the chemical phase separation and the size of this region at approaching the point of percolation of thulium ions on the lattice. Figure 1 shows frequency dependences of the real and

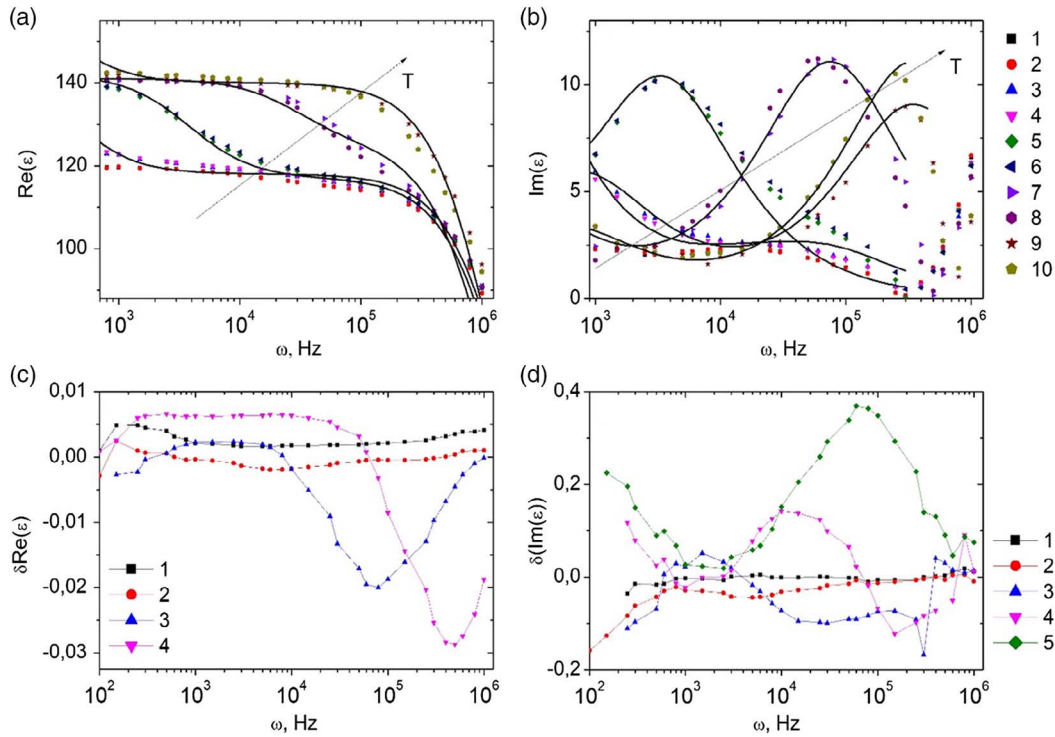


Figure 1. The a) real $\text{Re}(\epsilon)$ and b) imaginary $\text{Im}(\epsilon)$ parts of the permittivity of the sample $\text{Tm}_x\text{Mn}_{1-x}\text{S}$ with $x=0.05$ without field ($H=0$ kOe) at temperatures $T=300$ K (1), 350 K (3), 400 K (5), 450 K (7), 500 K (9) and in magnetic field $H=8$ kOe at temperatures $T=300$ K (2), 350 K (4), 400 K (6), 450 K (8), 500 K (10) versus the frequency ω . Solid lines: The permittivity in the Debye model. c) Magnetocapacitance $\delta\text{Re}(\epsilon)$ for sample $\text{Tm}_x\text{Mn}_{1-x}\text{S}$ with $x=0.05$ in magnetic field $H=8$ kOe at temperatures $T=350$ K (1), 400 K (2), 450 K (3), 500 K (4) versus frequency ω . d) The relative change of the imaginary part of the permittivity $\delta(\text{Im}(\epsilon))$ in magnetic field $H=8$ kOe at temperatures $T=300$ K (1), 350 K (2), 400 K (3), 450 K (4), 500 K (5) versus frequency ω .

imaginary parts of the permittivity at different temperatures. The $\epsilon(\omega)$ dependence consists of the low-frequency ($\omega < \omega_c$) and high-frequency ($\omega > \omega_c$) regions. In the low-frequency region $\epsilon(\omega)$ is described by the Debye model with the maximum dielectric loss

$$\text{Re}(\epsilon) = \epsilon_h + \frac{\chi_0}{1 + (\omega\tau_c)^2} + \frac{\sigma''}{\omega}; \quad \text{Im}(\epsilon) = \frac{\chi_0\omega\tau_c}{1 + (\omega\tau_c)^2} + \frac{\sigma'}{\omega} \quad (2)$$

where ϵ_h is the high-frequency contribution to the permittivity, χ_0 is the static susceptibility of dipoles, and $\sigma = \sigma' + i\sigma''$ is the complex electric conductivity of the regions with thulium ions. The $\text{Im}(\epsilon(\omega))$ maximum shifts to the high-frequency region upon heating, and the relaxation time found from the formula $\omega\tau_c = 1$ is described by the Arrhenius function $\tau_c = \tau_0 \exp(\Delta E/kT)$, where ΔE is the activation energy ($\Delta E = 0.55$ eV). In the high-frequency region ($\omega > \omega_c$), the complex permittivity depends linearly on frequency.

The dielectric loss is caused by the absorption and emission of phonons at the hopping of electrons. The imaginary part of the permittivity is related to the real part of the optical conductivity σ' as $\text{Im}(\epsilon) = \sigma''/\omega$. In disordered semiconductors with the hopping conductivity, the latter can have either the resonance or relaxation nature. If the energy of Coulomb repulsion of electrons separated by distance R is lower than the heat energy $e^2/\epsilon R \ll kT$, then the relaxation optical conductivity dominates^[11]

$$\sigma'(\omega) = \frac{1}{3} \pi^2 e^2 a g^2 \hbar \omega^2 R^4 \quad (3)$$

where a is the electron localization radius and g is the electron density of states at the Fermi level. In this case, we have $\text{Im}(\epsilon) = A\omega$. The frequency of the crossover ω_c from the Debye relaxation to the relaxation conductivity related to the absorption and emission of phonons is determined by the electron localization radius and electron density of states. If we assume that the electron is localized in the region of chemical phase separation induced by thulium ions and the electron localization radius is temperature-independent, then the growth of the ω_c value above 400 K is related to an increase in the electron density of states at the chemical potential level, $g \sim T^2$.

In a magnetic field, the Debye relaxation time increases, and the $\text{Re}(\epsilon)$ inflection point and the $\text{Im}(\epsilon)$ maximum shift toward lower frequencies. As a result, the permittivity decreases in a magnetic field at $\omega\tau = 1$ by 0.5%, 2.4%, and 3.3% at $T=400$, 450, and 500 K, respectively. The more significant changes were observed in the dielectric loss tangent, which depends on the enhancement of the electron scattering on local deformations and phonons in the thulium ion localization region. The dielectric loss increases by 14% and 36% at $T=450$ and 500 K and decreases to 15% in the low-frequency region at $T=350$ and 400 K for $x=0.05$.

Thulium and manganese sulfides are characterized by a metallic and semiconductors type of conductivity. When substituting manganese ions with thulium, the formation of a chemical electronic phase separation is possible, i.e., in the region of thulium ions, the conductivity increases. With increasing concentration, the size of the thulium ion cluster grows and, accordingly, the electron localization radius increases. **Figure 2** shows the components of the permittivity of the $\text{Tm}_x\text{Mn}_{1-x}\text{S}$ sample as functions of frequency for a concentration of $x = 0.1$. In these samples, the Debye and electron-phonon relaxation of the induced electric polarization is also implemented. Upon heating, the $\text{Im}(\epsilon)$ maximum shifts toward higher frequencies. The activation energy $\Delta E = 0.2 \text{ eV}$ (1550 cm^{-1}) is twice as low as at $x = 0.05$. The crossover frequency found from the $\text{Im}(\epsilon(\omega))$ minimum increases according to the power law $\omega_c \sim T^{3/2}$ during heating the sample. This is apparently related to the shift of the chemical potential with temperature and to the growth of the electron density $g \sim T^{3/4}$. In a magnetic field, the permittivity decreases and the maximum change $\delta\epsilon = 2.5\%$ is observed at $T = 450 \text{ K}$ (Figure 2d). The shift of the maximum of the imaginary component of the permittivity toward lower frequencies in a magnetic field leads to the change in the sign of the dielectric loss from positive $\delta(\text{Im}(\epsilon)) = 0.024$ to negative $\delta(\text{Im}(\epsilon)) = -0.08$ at $T = 450 \text{ K}$ (Figure 2c).

Mica sheets contain impurities that will also contribute to the change in magnetic permeability in a magnetic field.

The frequency dependence of mica was measured in the range 300–500 K without field and in a magnetic field of 12 kOe. The dispersion of the dielectric constant in the frequency range 10^2 – 10^6 Hz is 10% and increases by approximately the same value $\text{Re}(\epsilon) = 3.1$ – 3.6 with heating. Dielectric losses with increasing frequency decrease by an order of magnitude and are shown in the inset in **Figure 3b**. The dielectric constant and dielectric loss of mica are 50–100 times less than in the sample. In a magnetic field, the increase in the dielectric constant of mica is in the range $\Delta\epsilon = \epsilon(H) - \epsilon(0) = 0.006$ – 0.04 , and for sample $\text{Tm}_x\text{Mn}_{1-x}\text{S}$ with $x = 0.1$, the permeability decreases in the field $\Delta\epsilon = \epsilon(0) - \epsilon(H) = 0.3$ – 4 (Figure 2d).

The TmS and MnS compounds have the same NaCl-type crystal lattice, and the homogeneity region of the solutions of $\text{Tm}_x\text{Mn}_{1-x}\text{S}$ solutions is 20%. With increasing concentration of (X), the unit cell parameter increases linearly, which indicates the formation of $\text{Tm}_x\text{Mn}_{1-x}\text{S}$ solutions. In a face-centered cubic (fcc) lattice, the critical percolation concentration is $x_c = 2/z = 2/12 = 0.17$,^[12] where z is the number of nearest neighbors. Upon approaching the concentration $x_c = 0.17$ of percolation of thulium ions on the fcc lattice, the $\epsilon(\omega)$ dependence qualitatively changes (Figure 3). In the frequency range of 10^2 – 10^6 Hz , the permittivity cannot be described using the Debye model. The percolation of thulium ions on the lattice leads to shunting the capacitor plates and the absence of migration polarization at the interface between Mn and Tm ions.

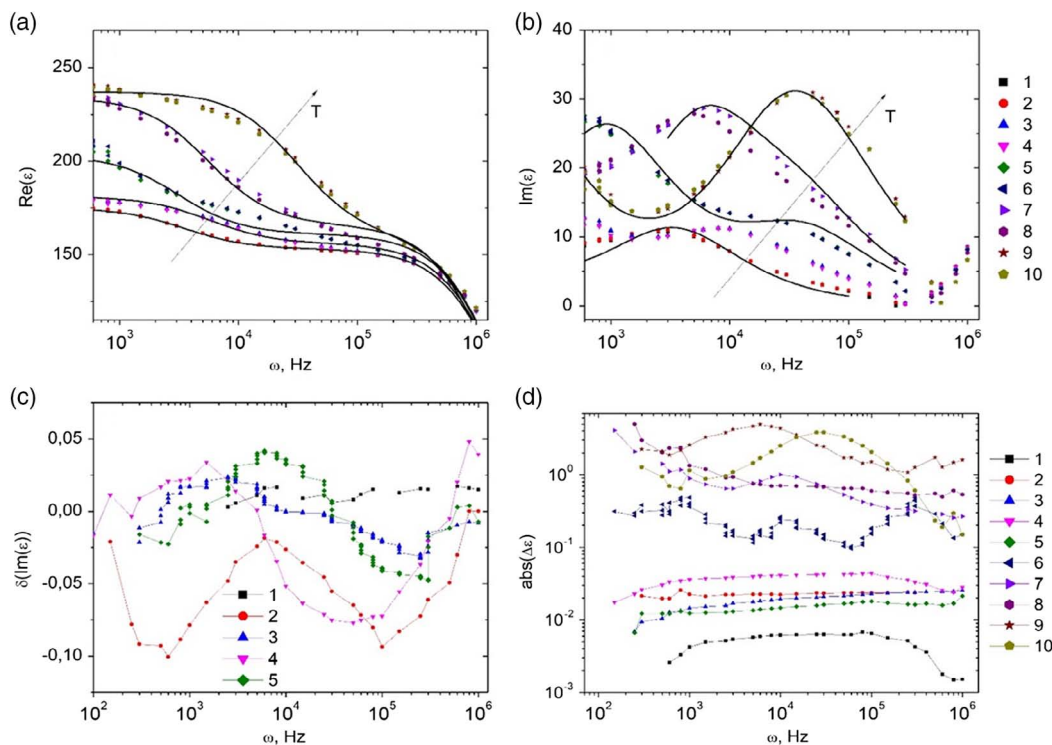


Figure 2. The a) real $\text{Re}(\epsilon)$ and b) imaginary $\text{Im}(\epsilon)$ parts of the permittivity of the sample $\text{Tm}_x\text{Mn}_{1-x}\text{S}$ with $x = 0.1$ without field ($H = 0 \text{ kOe}$) at temperatures $T = 300 \text{ K}$ (1), 350 K (3), 400 K (5), 450 K (7), 500 K (9) and in a magnetic field $H = 8 \text{ kOe}$ at temperatures $T = 300 \text{ K}$ (2), 350 K (4), 400 K (6), 450 K (8), 500 K (10) on the frequency ω . Solid lines: The permittivity in the Debye model. c) The relative change in the imaginary part of the permittivity $\delta(\text{Im}(\epsilon))$ in magnetic field $H = 8 \text{ kOe}$ at temperatures $T = 300 \text{ K}$ (1), 350 K (2), 400 K (3), 450 K (4), 500 K (5) on the frequency ω . d) Dependence of the absolute value (abs) of $\Delta\epsilon$ on the frequency ω for mica at temperatures $T = 300 \text{ K}$ (1), 350 K (2), 400 K (3), 450 K (4), 500 K (5) and for the sample $\text{Tm}_x\text{Mn}_{1-x}\text{S}$ with $x = 0.1$ at temperatures $T = 300 \text{ K}$ (6), 350 K (7), 400 K (8), 450 K (9), 500 K (10).

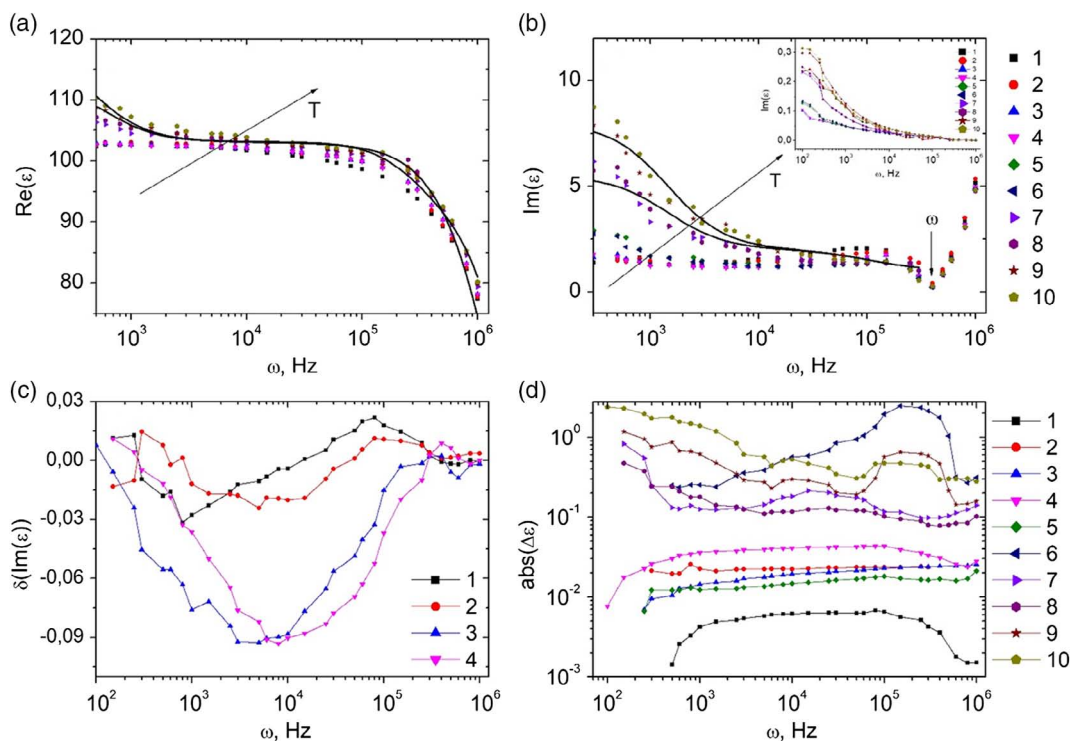


Figure 3. The a) real $\text{Re}(\epsilon)$ and b) imaginary $\text{Im}(\epsilon)$ parts of the permittivity of the sample $\text{Tm}_x\text{Mn}_{1-x}\text{S}$ with $x=0.15$ without field ($H=0$ kOe) at temperatures $T=300$ K (1), 350 K (3), 400 K (5), 450 K (7), 500 K (9) and in magnetic field $H=8$ kOe at temperatures $T=300$ K (2), 350 K (4), 400 K (6), 450 K (8), 500 K (10) on the frequency ω . Solid lines: The permittivity in the Debye model. Inset in (b): Dependence of $\text{Im}(\epsilon)$ on the frequency ω in the temperature range 300–500 K for mica. c) The relative change of the imaginary part of the permittivity $\delta(\text{Im}(\epsilon))$ in magnetic field $H=8$ kOe at temperatures $T=350$ K (1), 400 K (2), 450 K (3), 500 K (4) versus frequency ω . d) Dependence of $\text{abs}(\Delta\epsilon)$ on the frequency ω for mica at temperatures $T=300$ K (1), 350 K (2), 400 K (3), 450 K (4), 500 K (5) and for the sample $\text{Tm}_x\text{Mn}_{1-x}\text{S}$ with $x=0.15$ at temperatures $T=300$ K (6), 350 K (7), 400 K (8), 450 K (9), 500 K (10).

The $\epsilon(\omega)$ increase below 100 Hz is caused by the charge accumulation at the capacitor plates. The imaginary component of the permittivity decreases in a magnetic field to 9% at $T=450$ and 500 K due to a decrease in the conductivity $\sigma(H, \omega) < \sigma(0, \omega)$ (Figure 3c).

The frequency at which the permittivity is caused by the relaxation conductivity is temperature-independent. This is related to the stability of the electron density of states at the chemical potential level upon heating. At a concentration of $x=0.15$, the magnetic capacitance is positive and the permeability increases in the field (Figure 3d) ($\delta\epsilon < 0.01$). The electric polarization relaxation time and the frequency at which the permittivity is caused by the relaxation conductivity are shown in Figure 4.

Figure 5 shows infrared (IR) spectra for a concentration of $x=0.05$. Using these spectra, we found the frequency range where the transmission of the electromagnetic radiation sharply increases. The energy of the electromagnetic radiation quanta differs from the electron activation energy determined from the relaxation time by $50\text{--}80\text{ cm}^{-1}$. The intensity of the electromagnetic radiation transmission at a frequency of $\omega=4327\text{ cm}^{-1}$ increases upon heating and attains its maximum value at temperatures of 440–480 K. A scheme of the electronic transitions between the localized states of holes and electrons in the random potential is shown in Figure 5b. Under the action of

the IR radiation, the electron passes from the hole potential well to the electron potential well and tunnels to the nearest well with the further electronic transition to the chemical potential region. Thus, one of the electric polarization relaxation channels is the recombination of electron–hole pairs.

Our investigations of the effect of a magnetic field on the dielectric properties of the $\text{Tm}_x\text{Mn}_{1-x}\text{S}$ solid solution make it possible to explain the maximum magnetoimpedance $\Delta Z/Z=35\%$ ($x=0.05$), 6% ($x=0.1$), and 15% ($x=0.15$) at $T=450\text{ K}^{[10]}$ in this compound by the inductivity of the sample. The impedance Z (L, C) depends on the inductance and capacitance, which decreases smaller than the impedance by an order of magnitude in a magnetic field.

3. Conclusions

It was shown that the permittivity of $\text{Tm}_x\text{Mn}_{1-x}\text{S}$ in the frequency range to 1 MHz upon electron doping is caused by the migration polarization of localized electrons and the relaxation conductivity related to the emission and absorption of phonons. Using the Debye model, we found the relaxation time of the electric polarization, which has an activation nature and is described by the Arrhenius law. It was demonstrated that, in the vicinity of the concentration of percolation of thulium ions

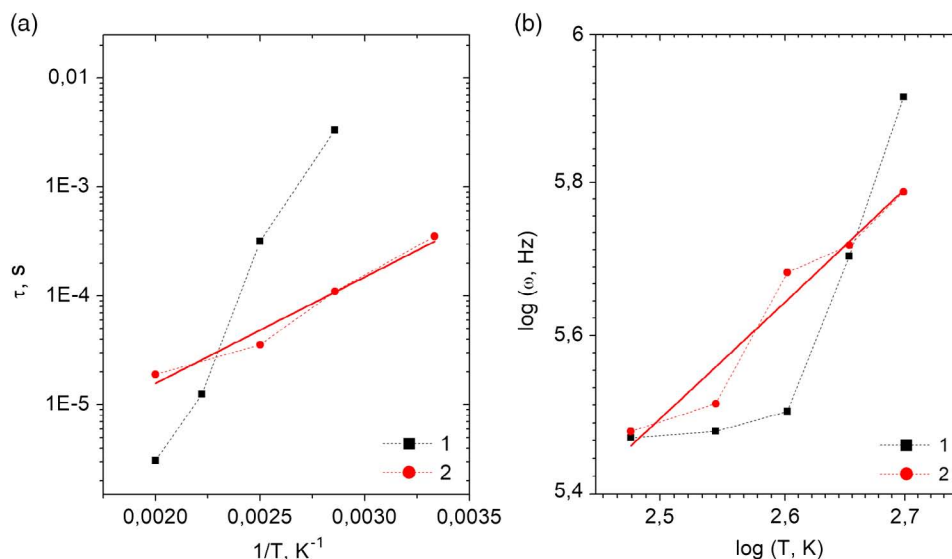


Figure 4. a) The relaxation time of migration polarization of $Tm_xMn_{1-x}S$ with $x=0.05$ (1), 0.1 (2) versus the inverse temperature. b) The crossover frequency from the migration polarization to the relaxation conductivity on the temperature in logarithmic coordinates for $Tm_xMn_{1-x}S$ with $x=0.05$ (1), 0.1 (2).

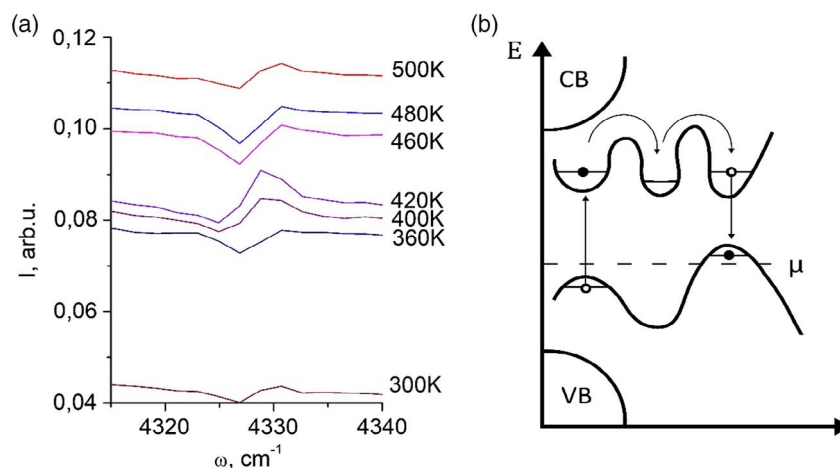


Figure 5. a) IR spectra of the $Tm_xMn_{1-x}S$ sample with $x=0.05$. b) Scheme of the electronic structure of $Tm_xMn_{1-x}S$, $x=0.05$. CB, conduction band; VB, valence band; μ , chemical potential, the random potential of impurity states.

in the lattice, the contribution of the migration polarization turns to zero and the dielectric characteristics are determined by the relaxation conductivity at high frequencies the range of which is temperature-independent. Using the IR spectroscopy investigations of $Tm_xMn_{1-x}S$, we established the channel of polarization relaxation via recombination of electron-hole pairs at low concentrations.

In a magnetic field, the permittivity of $Tm_{0.05}Mn_{0.95}S$ decreases by several percent for $T=350$ and 400 K and for $x=0.1$ at $T=450$ K. At a concentration of $x=0.15$, the magnetic capacitance is positive. The growth of the relaxation time in a magnetic field leads to the shift of the maximum dielectric loss toward lower frequencies and the change in the dielectric loss sign upon frequency variation in a magnetic field. The high

inductance of the sample in a magnetic field was found by comparing the magnetoimpedance and magnetic capacitance.

Acknowledgements

This study was supported by the Russian Foundation for Basic Research No. 18-32-00079 mol_a. The reported study was funded by Russian Foundation for Basic Research, Government of Krasnoyarsk Territory, Krasnoyarsk Regional Fund of Science No. 18-42-240001 r_a.

Conflict of Interest

The authors declare no conflict of interest.

Keywords

Debye model, infrared spectroscopy, magnetocapacitance, permittivity, relaxation time

Received: October 2, 2019

Revised: January 27, 2020

Published online: February 9, 2020

-
- [1] W. Eerenstein, N. D. Mathur, J. F. Scott, *Nature* **2006**, 442, 759.
[2] R. J. Zeches, M. D. Rossell, J. X. Zhang, A. J. Hatt, Q. He, C. H. Yang, *Science* **2009**, 326, 977.
[3] A. N. Spaldin, S.-W. Cheong, *Phys. Today* **2010**, 63, 38.
[4] A. P. Pyatakov, A. K. Zvezdin, *Usp. Fiz. Nauk* **2012**, 182, 593.
[5] J. C. Yang, Q. He, S. J. Suresha, C. Y. Kuo, C. Y. Peng, R. C. Haislmaier, M. A. Motyka, *Phys. Rev. Lett.* **2012**, 109, 247606.
[6] A. K. Zvezdin, A. P. Pyatakov, *Usp. Fiz. Nauk* **2009**, 179, 897.
[7] Y. Yamada, K. Kitsuda, S. Nohdo, N. Ikeda, *Phys. Rev. B* **2000**, 62, 12167.
[8] J. C. Maxwell, *Treatise on Electricity and Magnetism*, 3rd ed., Dover, New York, **1991**, pp. 5–531.
[9] M. M. Parish, P. B. Littlewood, *Phys. Rev. Lett.* **2008**, 101, 166602.
[10] S. S. Aplesnin, M. N. Sitnikov, A. M. Kharkov, A. N. Masyugin, V. V. Kretinin, O. B. Fisenko, M. V. Gorev, *Phys. Status Solidi B* **2019**, 256, 1900043.
[11] A. L. Efros, *Philos. Mag. B* **1981**, 43, 829.
[12] V. I. Belokon, K. V. Nefedev, *J. Exp. Theor. Phys.* **2001**, 69, 136.